PHYSICAL REVIEW LETTERS

# Anomalous Orbital-Energy Changes Observed during Spacecraft Flybys of Earth

John D. Anderson, James K. Campbell, John E. Ekelund, Jordan Ellis, and James F. Jordan

*Jet Propulsion Laboratory, California Institute of Technology, Pasadena, California 91109, USA*

We report and characterize anomalous orbital-energy changes observed during six Earth flybys by the Galileo, NEAR, Cassini, Rosetta, and MESSENGER spacecraft. These anomalous energy changes are consistent with an empirical prediction formula which is proportional to the total orbital energy per unit mass and which involves the incoming and outgoing geocentric latitudes of the asymptotic spacecraft velocity vectors. We use this formula to predict a potentially detectable flyby velocity increase of less than 1 mm/s for a second Rosetta flyby on November 13, 2007.

*Introduction.*—Between December 1990 and September 2005, deep-space missions were launched to Jupiter (Galileo mission), to an asteroid (NEAR mission), to a comet (Rosetta mission), to Saturn (Cassini mission), and to Mercury (MESSENGER mission). During flight, each of these missions was targeted to one or more flybys of Earth for purposes of either gaining or losing heliocentric orbital energy in order to reach their eventual target body [1]. When the first of these flybys, Galileo I, occurred on 8 December 1990, mission engineers at the Jet Propulsion Laboratory (JPL) noticed an unexpected frequency increase in the postencounter radio Doppler data generated by stations of the NASA Deep Space Network. Three of us (JDA, JKC, JFJ) studied this anomalous frequency shift during 1990–1993, but no explanation was found. A second flyby by the Galileo spacecraft exactly two years later (Galileo II) passed through the Earth's upper atmosphere at an altitude of about 300 km. Atmospheric drag prevented an unambiguous detection of a flyby anomaly [2]. Subsequently however, NEAR mission navigators at JPL [3] and Rosetta mission navigators at the European Space Operations Center (ESOC) in Darmstadt Germany [4] noticed anomalous frequency increases in the postencounter Doppler signals for those two flybys. The Cassini spacecraft also provided an Earth flyby. However, small thrusting maneuvers at the time of its closest approach obscured any immediate detection of an anomalous Doppler shift [5]. Finally, in August 2005, the MESSENGER spacecraft flew past Earth, but no anomaly was detected by the mission navigators [6].

We report here on results from a recent study involving the data analysis and interpretation of radio Doppler data from all six flybys. We find that there is indeed an anomalous energy change during Earth flybys on the order of $10^{-6}$, although we have been unable to find a physical cause or systematic error source for the anomaly. However, we have found an empirical prediction formula that fits all six flybys successfully. Its latitude dependence suggests that the Earth's rotation may be generating an effect much larger than the frame dragging effect of General Relativity, the Lense-Thirring effect [7]. Among all solar-system

bodies, the Earth provides the best natural laboratory for revealing anomalous effects, having both a relatively rapid rotation and a gravitational field well determined from artificial satellites [8].

*Analysis and empirical formula.*—The anomaly is most evident in Doppler and ranging data for the 1998 NEAR flyby, which was also the most asymmetrical about the equator. The *X*-band Doppler frequency data before closest approach can be fit to within the noise level of about 0.1 mm/s with a single numerically integrated trajectory (Fig. 1). The trajectory is well determined by 88 h of almost continuous Doppler data at a sample interval of
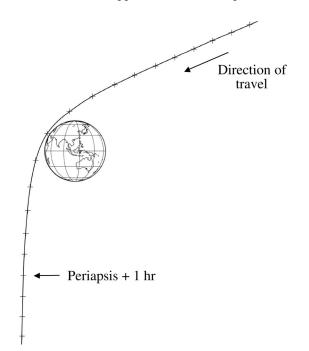


FIG. 1. Equatorial view of the NEAR flyby, the most asymmetrical flyby with respect to the Equator and the flyby with the largest energy change. The extent of the bending in the Earth's gravitational field, the geometry of the flyby and its time scale are illustrated. The tick marks are at 10-min intervals as measured from closest approach. Views of the five other flybys are similar and are not shown.

10 s. This preencounter trajectory can be extrapolated to times after closest approach and Doppler residuals can be computed without actually including the postencounter data in the fit. One would expect small residuals, especially for the data immediately after closest approach where the extrapolation interval is smallest. The gap in the data at closest approach, where the DSN stations are unable to track the spacecraft, is 3 h, 39 m. The expected Doppler extrapolation error over this gap is at most 1 mm/s.

Unexpectedly, the postencounter residuals are offset by about 13.5 mm/s from the preencounter residuals, as shown in Fig. 2. In addition, an approximately diurnal sinusoidal signal is evident in the extrapolated residuals. This sinusoid is caused by an inability of the preencounter data to predict the direction of the postencounter velocity vector to sufficient accuracy. Other tests, such as fitting the postencounter data and extrapolating to the preencounter data, show that the pre and postencounter trajectories are inconsistent. This inconsistency is not limited to the Doppler data. When the ranging data is differenced and compared to the Doppler data, exactly the same inconsistency is observed. Doppler data is a measure of the frequency shift in the carrier wave, while ranging data is determined by the time delay in a ranging phase modulation applied to the carrier wave at the transmitting station.

We have characterized this anomalous behavior, observed in both data types, by the difference in osculating Kepler orbital elements in two trajectories, one that fits the preencounter Doppler data to the noise level and another that fits the postencounter Doppler data to the noise level. The position vector **r** and velocity vector **v** that result from the numerically integrated trajectories can be converted to osculating orbital elements. In particular, the hyperbolic excess velocity $V_\infty$ and the incoming and outgoing asymptotic velocity vectors are defined as osculating elements by this technique. The resulting osculating elements for the

six available flybys are tabulated in Table I, along with the observed anomalous increase in $V_\infty$ for each flyby. The osculating value of $V_\infty$ is plotted in Fig. 3(a) for NEAR by means of the expression,

$$V_\infty^2 = \mathbf{v} \cdot \mathbf{v} - \frac{2\mu}{r}, \qquad (1)$$

where $\mu$ (398 600.4 km$^3$/s$^2$) is the gravitational constant times the mass of the Earth and $r$ is the magnitude of **r**. The osculating $V_\infty$ varies from about 6.87 km/s to about 6.83 km/s over the entire data interval, largely because of trajectory perturbations by the sun and moon. However, the variation in the difference of the two values of the $V_\infty$ between the postencounter Doppler-fitted trajectory and the preencounter Doppler-fitted trajectory is only about 0.05 mm/s, as shown in Fig. 3(b). We determine the value of $\Delta V_\infty$ for NEAR at closest approach with a standard error of $\pm 0.01$ mm/s, as shown in Table I, where the error is determined by the accuracy of the pre- and postencounter fitted trajectories, not by the time variability of $\Delta V_\infty$ over the total Doppler data interval.

Our prediction formula can be expressed in its simplest form in terms of the respective declinations $\delta_i$ and $\delta_o$ of the incoming and outgoing osculating asymptotic velocity vectors, or effectively in terms of the geocentric latitudes. The arcane difference between geocentric latitude and inertial declination is not statistically significant. The prediction formula can be written as

$$\frac{\Delta V_\infty}{V_\infty} = \frac{1}{2}\frac{\Delta E}{E} = K(\cos\delta_i - \cos\delta_o). \qquad (2)$$

The change represented by $\Delta V_\infty$, or, equivalently, total specific energy $\Delta E$, represents the postencounter orbital conditions minus the preencounter conditions, which according to conventional physics should agree. We observe that the proportionality coefficient $K$ in the formula can be
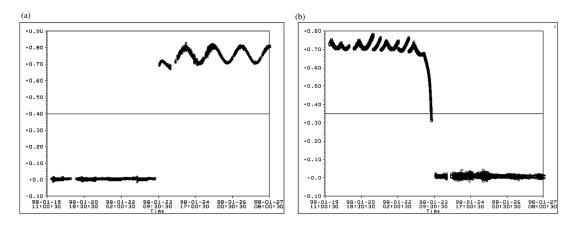


FIG. 2.   $X$-band Doppler residuals in the sense observed Doppler frequency shift minus calculated Doppler frequency shift in units of Hz [10] from separately fitting (a) the pre- and (b) the postencounter data for the NEAR flyby. The residuals cluster on opposite sides of the respective fits and demonstrate the impossibility of fitting both pre- and postencounter data with a single fit. The difference in Doppler frequency shift is approximately 0.760 Hz, consistent with an increase of 13.5 mm/s in the $V_\infty$ needed to fit both sides of the encounter.

TABLE I.   Earth flyby parameters at closest approach for Galileo, NEAR, Cassini, Rosetta, and MESSENGER (M'GER) spacecraft. The altitude $H$ is referenced to an Earth geoid, the geocentric latitude $\phi$ and longitude $\lambda$ are listed for the closest approach location, $V_f$ is the inertial spacecraft velocity at closest approach, $V_\infty$ is the osculating hyperbolic excess velocity, the deflection angle (DA) is the angle between the incoming and outgoing asymptotic velocity vectors, the angle $I$ is the inclination of the orbital plane on the Earth's equator, the next four rows represent the right ascension $\alpha$ and declination $\delta$ of the incoming (i) and outgoing (o) osculating asymptotic velocity vectors, and $M_{SC}$ is a best estimate of the total mass of the spacecraft during the encounter. The last three rows of the table give the measured change in $V_\infty$, the estimated realistic error in $\Delta V_\infty$, and the prediction of $\Delta V_\infty$ by Eq. (1). The measured $\Delta V_\infty$ for GLL-II is actually—8 mm/s, but it is reduced in magnitude after subtracting out an estimated atmospheric drag of $-3.4$ mm/s.

| Parameter | GLL-I | GLL-II | NEAR | Cassini | Rosetta | M'GER |
|---|---|---|---|---|---|---|
| Date | 12/8/90 | 12/8/92 | 1/23/98 | 8/18/99 | 3/4/05 | 8/2/05 |
| $H$ (km) | 960 | 303 | 539 | 1175 | 1956 | 2347 |
| $\phi$ (deg) | 25.2 | $-33.8$ | 33.0 | $-23.5$ | 20.20 | 46.95 |
| $\lambda$ (deg) | 296.5 | 354.4 | 47.2 | 231.4 | 246.8 | 107.5 |
| $V_f$ (km/s) | 13.740 | 14.080 | 12.739 | 19.026 | 10.517 | 10.389 |
| $V_\infty$ (km/s) | 8.949 | 8.877 | 6.851 | 16.010 | 3.863 | 4.056 |
| DA (deg) | 47.7 | 51.1 | 66.9 | 19.7 | 99.3 | 94.7 |
| $I$ (deg) | 142.9 | 138.7 | 108.0 | 25.4 | 144.9 | 133.1 |
| $\alpha_i$ (deg) | 266.76 | 219.35 | 261.17 | 334.31 | 346.12 | 292.61 |
| $\delta_i$ (deg) | $-12.52$ | $-34.26$ | $-20.76$ | $-12.92$ | $-2.81$ | 31.44 |
| $\alpha_o$ (deg) | 219.97 | 174.35 | 183.49 | 352.54 | 246.51 | 227.17 |
| $\delta_o$ (deg) | $-34.15$ | $-4.87$ | $-71.96$ | $-4.99$ | $-34.29$ | $-31.92$ |
| $M_{SC}$ (kg) | 2497 | 2497 | 730 | 4612 | 2895 | 1086 |
| $\Delta V_\infty$ (mm/s) | 3.92 | $-4.6$ | 13.46 | $-2$ | 1.80 | 0.02 |
| $\sigma_{V_\infty}$ (mm/s) | 0.3 | 1.0 | 0.01 | 1 | 0.03 | 0.01 |
| Equation (1) (mm/s) | 4.12 | $-4.67$ | 13.28 | $-1.07$ | 2.07 | 0.06 |

expressed in terms of the Earth's angular rotational velocity $\omega_E$ of $7.292\,115 \times 10^{-5}$ rad/s [9], its mean radius $R_E$ of 6371 km [9] and speed of light $c$ by

$$K = \frac{2\omega_E R_E}{c} = 3.099 \times 10^{-6} \quad (3)$$

*Data processing.*—Our results were produced at JPL using the Orbit Determination Program (ODP). Calculations using ODP for analysis of the Galileo I Doppler data were duplicated in 1991 by software at the

Goddard Space Flight Center and at the University of Texas. The ODP results reported here for Rosetta match those produced at ESA by navigators using their software. Doppler frequency shift is defined as the difference of cycle count at a predetermined Doppler integration time TC divided by TC and referenced to a time-variable uplink frequency, as recorded by the transmitting station [10].

Lämmerzahl *et al.* [11] studied and dismissed a number of possible explanations for the Earth flyby anomalies, including Earth atmosphere, ocean tides, solid Earth tides,
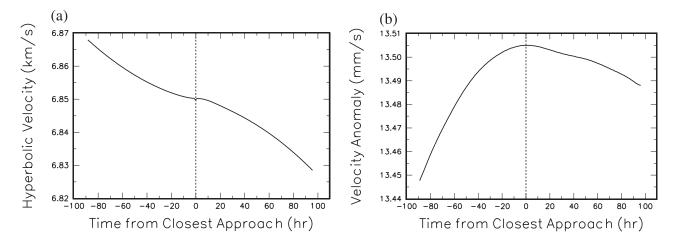


FIG. 3.   Panel (a) shows the osculating hyperbolic excess velocity $V_\infty$ for the NEAR flyby. Panel (b) shows the difference in osculating $V_\infty$ between the best-fit trajectory for Doppler data taken after closest approach minus the best-fit trajectory for Doppler data taken before closest approach. The osculating parameters are evaluated over the entire data interval from minus 88.4 h to plus 95.6 h.

spacecraft charging, magnetic moments, Earth albedo, solar wind, coupling of Earth's spin with rotation of the radio wave, Earth gravity, and relativistic effects predicted by Einstein's theory. All these potential sources of systematic error, and more, are modeled in the ODP. None can account for the observed anomalies.

*Conclusions.*—Like the Pioneer anomaly [12], and perhaps even more surprising, the Earth flyby anomaly is a real effect inherent to the tracking of spacecraft. Its source is unknown. We expect to continue efforts to understand the anomaly by characterizing the behavior of other orbital parameters of the flybys, including the 2007 Rosetta flyby. For example, the specific orbital angular momentum of the flybys and the angular deflection of $V_\infty$ will be included in our future work.

---

[1] A preliminary discussion of these flybys appeared in J. D. Anderson, J. K. Campbell, and M. M. Nieto, New Astron. Rev. **12**, 383 (2007); a discussion of the technique of using a flyby to gain or lose orbital energy can be found in G. A. Flandro, Astronaut. Acta **12**, 329 (1966); J. A. Van Allen, Am. J. Phys. **71**, 448 (2003).

[2] C. Edwards, J. Anderson, P. Beyer, S. Bhaskaran, J. Border, S. DiNardo, W. Folkner, R. Haw, S. Nandi, F. Nicholson, T. Ottenhoff, and S. Stevens, Adv. Astron. Sci. **85**, 1609 (1994).

[3] P. G. Antreasian and J. R. Guinn, AIAA Paper No. 98-4287 presented at the AIAA/AAS Astrodynamics Specialist Conference and Exhibit (Boston, August 10-12, 1998), and available at http://www2.aiaa.org/citations/mp-search.cfm (1998).

[4] T. Morley and F. Budnik, *Proceedings of the International Symposium on Space Technology and Science*, Vol. 25, p. 593, (2006).

[5] M. D. Guman, D. C. Roth, R. Ionasescu, T. D. Goodson, A. H. Taylor, and J. B. Jones, Advances in Astronautical Sciences **105**, 1053 (2000).

[6] B. Williams, A. Taylor, E. Carranza, J. Miller, D. Stanbridge, B. Page, D. Cotter, L. Efron, R. Farquhar, J. McAdams, and D. Dunham, Adv. Astron. Sci. **120**, 1233 (2005).

[7] J. Lense and H. Thirring, Phys. Z. **19**, 156 (1918).

[8] B. D. Tapley, S. Bettadpur, M. Watkins, and C. Reigber, Geophys. Res. Lett. **31**, L09 607 (2004).

[9] F. D. Stacey, *Physics of the Earth, Appendix A* (Brookfield Press, Brisbane, Australia, 1992), 3rd ed.

[10] T. D. Moyer, *Formulation for Observed and Computed Values of Deep Space Network Data Types for Navigation*, JPL Deep-Space Communications and Navigation Series (Wiley-Interscience, Hoboken, NJ, 2003).

[11] C. Lämmerzahl, O. Preuss, and H. Dittus, arXiv:gr-qc/0604052.

[12] An announcement of the Pioneer Anomaly appeared in J. D. Anderson, P. A. Laing, E. L. Lau, A. S. Liu, M. M. Nieto, and S. G. Turyshev, Phys. Rev. Lett. **81**, 2858 (1998); A detailed technical description, including an error budget, appeared in J. D. Anderson, P. A. Laing, E. L. Lau, A. S. Liu, M. M. Nieto, and S. G. Turyshev, Phys. Rev. D **65**, 082004 (2002).